Critical Temperature Sensor Based on Spiking Neuron Models: Experimental Results with Discrete MOS Circuits

Gessyca Maria Tovar, Tetsuya Hirose, Tetsuya Asai, and Yoshihito Amemiya

Graduate School of Information Science & Technology, Hokkaido University

Kita 14, Nishi 9, Kita-ku, Sapporo, 060-0814, Japan

Email: gessyca@sapiens-ei.eng.hokudai.ac.jp, hirose@sapiens-ei.eng.hokudai.ac.jp, asai@sapiens-ei.eng.hokudai.ac.jp, amemiya@sapiens-ei.eng.hokudai.ac.jp

Abstract.
A temperature sensor, which can be implemented on monolithic CMOS IC was proposed [1]. The circuit consist of subthreshold CMOS circuits whose dynamical behavior changes at a given threshold temperature i.e. switches to and from oscillatory and stationary behaviors. The circuit operation was investigated through theoretical analysis and numerical simulations using Simulation Program of Integrated Circuit Emphasis (SPICE). In this paper we demonstrate the operation of the proposed circuit by using discrete MOS devices through experimental results.

1. Introduction

Temperature is the most often-measured environmental quantity. This might be expected since temperature control is fundamental in electronic and other systems. There are several temperature sensing techniques. The most common are RTDs (resistive-temperature detectors), thermocouples, thermistors, and silicon temperature sensors [2]. Among the present temperature sensors, a thermistor that has positive temperature coefficient (PTC) is widely used because it exhibits a sharp increase of its resistance at a specific temperature. Therefore, PTC thermistors are suitable for implementation in temperature control systems that make decisions, such as over temperature shutdown, turn on/off cooling fan, or general purpose temperature monitor.

Temperature characteristic of PTC thermistors made of ceramic, are based on its material characteristic and its relative proportions [2], [3]. Hence, during the soldering process, the electrical resistivities of PTCs are shifted by a phenomenon called leaching. In addition, leaching causes degradation of the solder-electrode and the electrode-semiconductor bond, this may result in thermistor having reduced its stability and reliability. To avoid these post-manufacture effects, we made a critical temperature sensor [1] with a sharp transition characteristic similar to PTC and inspired by biological neurons which can be implemented on monolithic CMOS IC. In this paper we confirmed the operation of the circuit by using discrete MOS devices through experimental results.

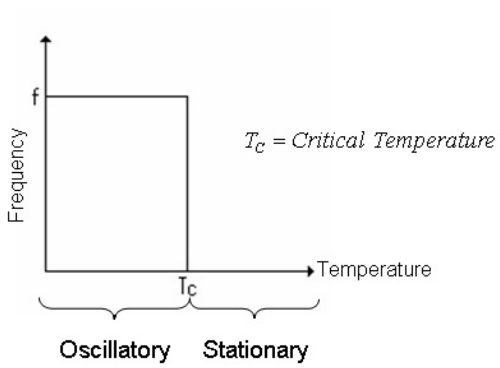

Fig. 1: Critical temperature sensor operation model

2. The Model

Figure 1 shows the temperature sensor operation model. It consists of a nonlinear oscillator that changes its state between oscillatory and stationary when it receives an external perturbation. The key idea is the used of excitable circuits that are strongly inspired by biological neuron's operation. Temperature increase causes a regular and reproducible increase in the frequency of pacemaker potential in most *Aplysia* and *Helix* excitable neurons [4]. In other words, excitable neurons can be used as sensors to determine the temperature range in a natural environment. The model is based on the Wilson-Cowan system [5] because of ease of theoretical analysis and subthreshold CMOS implementation.

2.1. Critical Temperature Sensor Circuit

Figure 2 shows the proposed circuit, the sensor section consists of two pMOS differential pairs (M_1-M_2 and M_3-M_4) operating in their subthreshold region. For the operation of the circuit external components are required, these components consist of, two capacitors (C_1 and C_2), two off-chip metal-film resistors (g). Also for the experimental results two current mirrors were used as the bias current of differential pairs. It is important to denote that for the final implementation of the critical temperature sensor a current reference circuit with low-temperature dependence [6] should be used.

Differential pairs subthreshold current I_1 and I_2 are

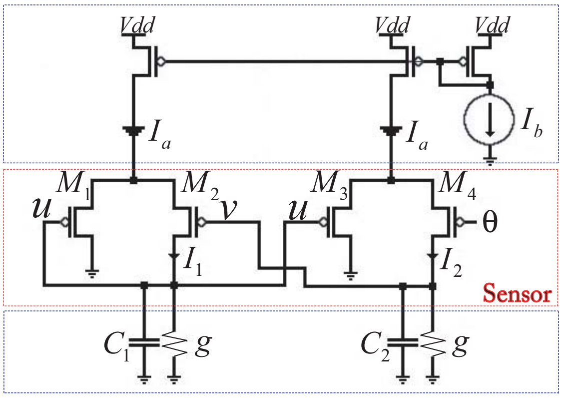

Fig. 2: Critical temperature sensor circuit.

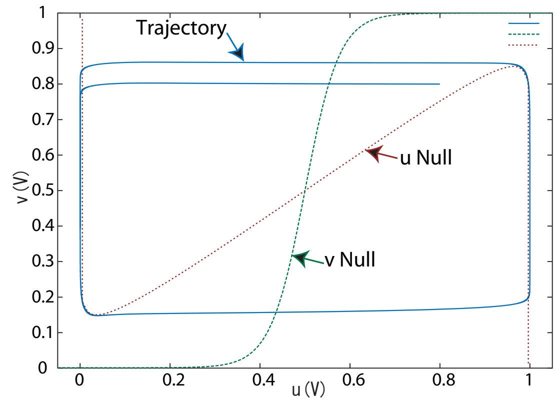

Fig. 3: Trajectory and nullclines simulation results at 27 ℃.

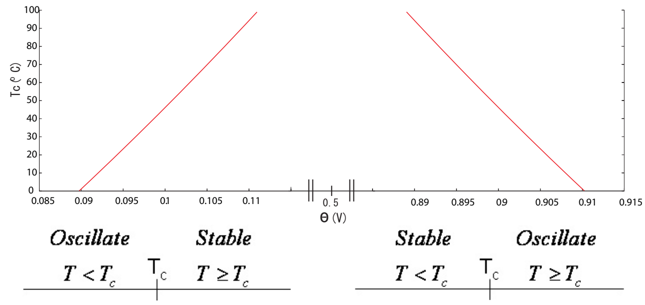

Fig. 4: Relation between $\theta_{\pm}$ and T_c simulation results.

given by:

$$I_1 = I_a \frac{e^{\kappa u / v_T}}{e^{\kappa u / v_T} + e^{\kappa v / v_T}} \quad (1)$$

and

$$I_2 = I_a \frac{e^{\kappa u / v_T}}{e^{\kappa u / v_T} + e^{\kappa \theta / v_T}}, \quad (2)$$

the circuit dynamics can be determined by applying Kirchhoff's Current Law to both differential pairs, which is represented as follows:

$$C_1 \dot{u} = -gu + \frac{I_a e^{\kappa u / v_T}}{e^{\kappa u / v_T} + e^{\kappa v / v_T}} \quad (3)$$

and

$$C_2 \dot{v} = -gv + \frac{I_a e^{\kappa u / v_T}}{e^{\kappa u / v_T} + e^{\kappa \theta / v_T}}, \quad (4)$$

where, κ is subthreshold slope, v_T is thermal voltage (v_T = KT/q), K is Boltzmann's constant, T is temperature, q is elementary charge, C_1 and C_2 are the capacitance, they represent the time constants, and θ is bias voltage.

The threshold temperature T_c can be set to a desire value by adjusting an external bias voltage (θ). The circuit changes its dynamical behavior i.e. oscillatory or stationary behaviors, with its operation temperature and the bias voltage conditions. At temperatures lower than T_c the circuit oscillates, but the circuit is stable (do not oscillate) at temperatures higher than T_c.

3. Simulations and Experimental Results

Numerical simulations were conducted by setting C_1 and C_2 at 0.1 and 10 pF, respectively, g was set at 1 nS, and reference current I_b at 1 nA. Figure 3 shows the nullclines and trajectory of the circuit with θ set at 0.5 V and T set at 27 ℃; the system is in an oscillatory state. Setting T_c and changing θ until the system changes its state. We established a numerical relation between T_c and θ : θ_- for ***u*** and ***v*** local minimums and θ_+ for ***u*** and ***v*** local maximums. Figure 4 shows the relation between $\theta_{\pm}$ and T_c. When θ_- is used to set T_c, the system is stable at temperatures higher than T_c; while when θ_+ is used, the system is stable when the temperature is lower than T_c and oscillatory when it is higher than T_c.

Also we confirmed the critical temperature sensor operation using discrete MOS circuits through experimental results. Parasitic capacitances and a capacitance of 0.033 μ F were used for C_1 and C_2 respectively, the resistances (g) were set to 10 MΩ. The input current of current mirrors was set to 100 nA and we obtained the output current of 78 nA. Measures at room temperature were made. With the bias voltage (θ) set to 500 mV measures of voltage at ***u*** and ***v*** were made, with these conditions the circuit was oscillating. Also measures of voltage at ***u*** and ***v*** for different values of θ were made. The results showed that for values of θ lower than 170 mV the circuit did not oscillate (was stable), but for values higher than 170 mV the circuit

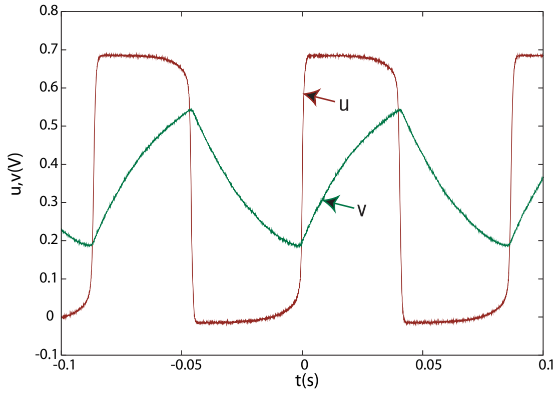

Fig. 5: Oscillatory state θ =170 mV at room temperature.

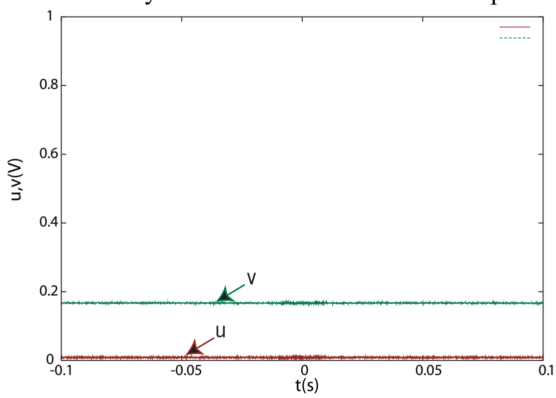

Fig. 6: Stationary state θ =150 mV at room temperature.

becomes oscillatory. Figure 5 and 6 shows the oscillatory and stable states of $\boldsymbol{u}$ and $\boldsymbol{v}$ with θ set to 170 mV and 150 mV respectively. Furthermore, measures of the nullclines (steady state voltage of differential pair) were made. The $\boldsymbol{v}$ nullcline (steady state voltage $\boldsymbol{v}$ of differential pair M_3-M_4), was measured by applying a variable DC voltage (from 0 to 1 V) on $\boldsymbol{u}$ and measuring the voltage on $\boldsymbol{v}$. For the measure of the $\boldsymbol{u}$ nullcline (steady state voltage $\boldsymbol{u}$ of differential pair M_1-M_2) a special configuration of the first differential pair of the circuit was used, fig. 7 shows the circuit used for $\boldsymbol{u}$ nullcline measurement. On the same way as $\boldsymbol{v}$ nullcline by applying a variable DC voltage (from 0 to 1 V) on $\boldsymbol{v}$, and measuring the voltage on $\boldsymbol{u_o}$ and $\boldsymbol{u_1}$ we could obtain the $\boldsymbol{u}$ nullcline by graphing the points where $\boldsymbol{u_o}$ and $\boldsymbol{u_1}$ had the same value. The results that we obtained were a series of points showing the shape of the $\boldsymbol{u}$ nullcline. The series of points was divided on three sections and the average was calculated showing the $\boldsymbol{u}$ nullcline. Figure 8 shows the $\boldsymbol{u}$ nullcline divided on the three sections used for the average calculation. Figure 9 shows the trajectory and nullclines of the circuit obtained with experimental results and with θ set to 500mV.

Measures at different temperatures were made. By setting the bias voltage θ to a fixes value and changing

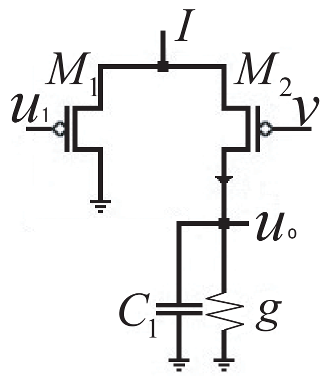

Fig. 7: Circuit for calculation of $\boldsymbol{u}$ nullcline

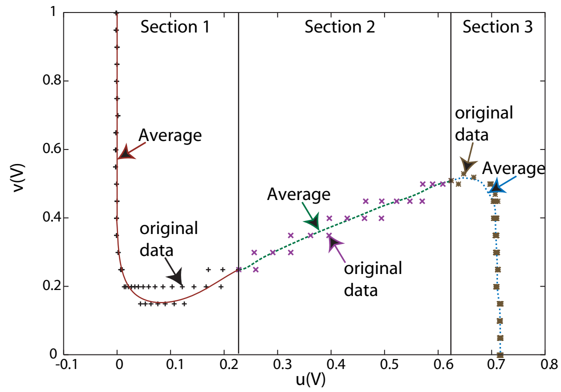

Fig. 8: Sections used for $\boldsymbol{u}$ nullcline calculation.

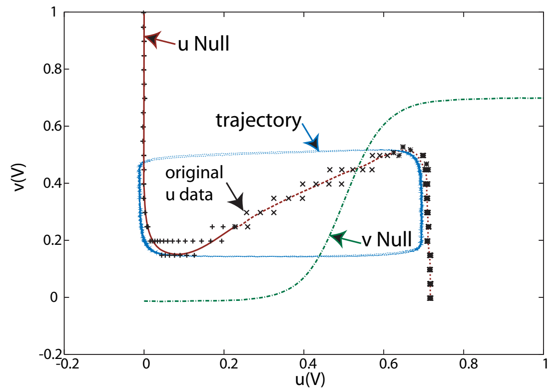

Fig. 9: Experimental nullclines and trajectory.

the external temperature to find the value of the critical temperature T_c where the circuit changes from one state to the other. With the bias voltage θ set at 170 mV at room temperature (T = 23 ℃) the circuit was oscillating, when the temperature increases to (T = 26 ℃) the circuit changed its state to stationary (did not oscillate). Once again when temperature decreases one degree (T = 25 ℃) the circuit started to oscillate. Hence the critical temperature was (T_c = 26 ℃). Measures of critical temperature T_c for different were θ made. In order to compare experimental results with theoretical ones, the actual κ (subthreshold slope) of the discrete MOS devices was measured and found to be in the order of 0.1.

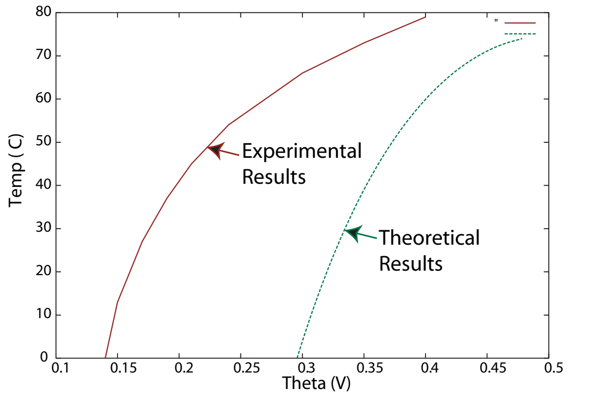

Fig. 10: Bias voltage vs Temperature, experimental results.

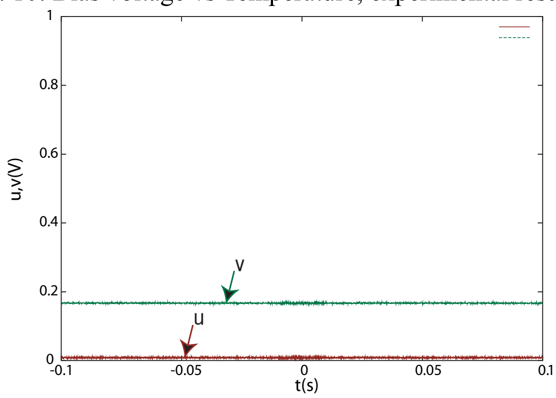

Fig. 11: Stationary state with $\theta = 140$ mV and T = 23 ℃

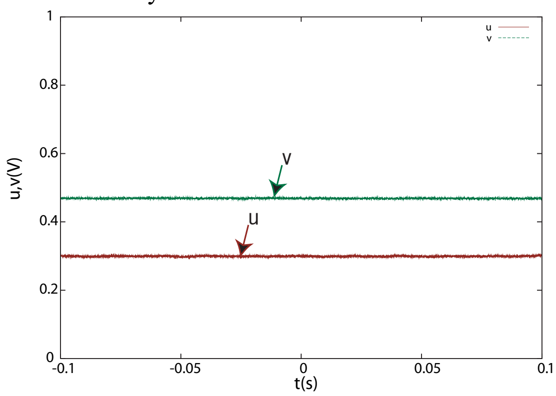

Fig. 12: Stationary state with $\theta = 140$ mV and T = 75 ℃

Figure 10 shows the critical temperature for each θ compared with the critical temperature obtained through theoretical analysis. The graphic shows a curve with positive slope in both cases. This is because the temperature difference between one value for the bias voltage and the other decreases as the bias voltage increases. So, on experimental results for a $\theta = 140$mV and $\theta = 150$mV the critical temperature T_c are 0 ℃ and 13 ℃ respectively, the difference of temperature is 13 ℃. For a $\theta = 240$mV and $\theta = 250$mV the critical temperature T_c are 54 ℃ and 56 ℃ respectively, the difference of temperature is only 2 ℃. The difference between the experimental results and the theoretical results is due to the leak current produce by plastic diode present between the source and well of discrete MOS devices. Also, because of the leak current on discrete MOS devices, when temperature increases the stable voltage of ***u*** and ***v*** of the circuit also increases. Figure 11 and 12 shows the stationary state with θ set to 140 mV and temperature set to 23 ℃ and 75 ℃ respectively.

5. Summary

A critical temperature sensor, which can be implemented on monolithic CMOS IC was proposed. The operation of the circuit was verified by using discrete MOS devices through experimental results. The threshold temperature T_c was set to a desire value by adjusting the external bias voltage (θ). The circuit changed its state between oscillatory and stationary when the external temperature was lower or higher than the critical temperature T_c.

6. References

[1] Tovar G. M., Hirose T., Asai T., and Amemiya Y., "Critical temperature sensor based on spiking neuron models," Proceedings of the *2006 International Symposium on Nonlinear Theory and its Applications*, pp. 84-88, Bologna, Italy (Sep. 11-14, 2006).

[2] W. Gopel, J. Hesse, and J. N. Zermel, *Sensors. A comprehensive survey,* Vol. 4, VCH, *Thermal sensors* (T. Ricolfi and J. Scholz, Eds.), 1990, pp. 235–239.

[3] C. C. Wang, S. A. Akbar, and M. J. Madou, “Ceramic based resistive sensors,” J. Electroceramics, Vol. 2, No. 4, pp. 273–282, 1998.

[4] D. S. Fletcher and L. J. Ram, “High temperature induces reversible silence in Aplysia R15 bursting pacemaker neuron,” Comp. Biochem. Physiol., Vol. 98A, pp. 399–405, 1990.

[5] H. R. Wilson and J. D. Cowan, Excitatory and inhibitory interactions in localized populations of model neurons, *Biophys. J.*, Vol. 12, pp. 1–24, 1972.

[6] T. Hirose, T. Matsuoka, K. Taniguchi, T. Asai, and Y. Amemiya, "Ultralow-power current reference circuit with low-temperature dependence," IEICE Transactions on Electronics, Vol. E88-C, No. 6, pp. 1142–1147 (2005).